

## Original Article



## OPEN ACCESS

**Received:** May 2, 2023  
**Revised:** Jun 6, 2023  
**Accepted:** Jun 19, 2023  
**Published online:** Aug 3, 2023

### \*Correspondence to

#### Sang Sun Yoon

Department of Microbiology and Immunology,  
Yonsei University College of Medicine, 50-1  
Yonsei-ro, Seodaemun-gu, Seoul 03722, Korea.  
Email: sangsun\_yoon@yuhs.ac

#### Hyun Jik Kim

Department of Otorhinolaryngology, Seoul  
National University College of Medicine, 101  
Daehak-ro, Jongno-gu, Seoul 03080, Korea.  
Email: hyunjerry@snu.ac.kr

#### Ho-Keun Kwon

Department of Microbiology and Immunology,  
Yonsei University College of Medicine, 50-1  
Yonsei-ro, Seodaemun-gu, Seoul 03722, Korea.  
Email: hk@yuhs.ac

Copyright © 2023. The Korean Association of  
Immunologists

This is an Open Access article distributed  
under the terms of the Creative Commons  
Attribution Non-Commercial License (<https://creativecommons.org/licenses/by-nc/4.0/>)  
which permits unrestricted non-commercial  
use, distribution, and reproduction in any  
medium, provided the original work is properly  
cited.

### ORCID iDs

Gwanghee Kim <https://orcid.org/0009-0008-0884-8918>  
Yoojin Lee <https://orcid.org/0000-0003-3895-9236>  
Jin Sun You <https://orcid.org/0009-0006-9958-473X>

<https://immunenetw.org>

# A Moonlighting Protein Secreted by a Nasal Microbiome Fortifies the Innate Host Defense Against Bacterial and Viral Infections

Gwanghee Kim <sup>1,2,3</sup>, Yoojin Lee <sup>1,2</sup>, Jin Sun You <sup>1,2</sup>, Wontae Hwang <sup>1,2</sup>,  
Jeewon Hwang <sup>1,2</sup>, Hwa Young Kim <sup>1,2</sup>, Jieun Kim <sup>1,4</sup>, Ara Jo <sup>5,6</sup>, In ho Park <sup>1,4</sup>,  
Mohammed Ali <sup>1,2</sup>, Jongsun Kim <sup>1,4</sup>, Jeon-Soo Shin <sup>1,2,4,7</sup>, Ho-Keun Kwon <sup>1,2,4,\*</sup>,  
Hyun Jik Kim <sup>5,6,\*</sup>, Sang Sun Yoon <sup>1,2,3,4,7,\*</sup>

<sup>1</sup>Department of Microbiology and Immunology, Yonsei University College of Medicine, Seoul 03722, Korea  
<sup>2</sup>Brain Korea 21 PLUS Project for Medical Sciences, Yonsei University College of Medicine, Seoul 03722, Korea  
<sup>3</sup>BioMe Inc., Seoul 02455, Korea  
<sup>4</sup>Institute for Immunology and Immunological Diseases, Yonsei University College of Medicine, Seoul 03722, Korea  
<sup>5</sup>Department of Otorhinolaryngology, Seoul National University College of Medicine, Seoul 03080, Korea  
<sup>6</sup>Sensory Organ Research Institute, Seoul National University Medical Research Center, Seoul 03080, Korea  
<sup>7</sup>Severance Biomedical Science Institute, Yonsei University College of Medicine, Seoul 03722, Korea

## ABSTRACT

Evidence suggests that the human respiratory tract, as with the gastrointestinal tract, has evolved to its current state in association with commensal microbes. However, little is known about how the airway microbiome affects the development of airway immune system. Here, we uncover a previously unidentified mode of interaction between host airway immunity and a unique strain (AIT01) of *Staphylococcus epidermidis*, a predominant species of the nasal microbiome. Intranasal administration of AIT01 increased the population of neutrophils and monocytes in mouse lungs. The recruitment of these immune cells resulted in the protection of the murine host against infection by *Pseudomonas aeruginosa*, a pathogenic bacterium. Interestingly, an AIT01-secreted protein identified as GAPDH, a well-known bacterial moonlighting protein, mediated this protective effect. Intranasal delivery of the purified GAPDH conferred significant resistance against other Gram-negative pathogens (*Klebsiella pneumoniae* and *Acinetobacter baumannii*) and influenza A virus. Our findings demonstrate the potential of a native nasal microbe and its secretory protein to enhance innate immune defense against airway infections. These results offer a promising preventive measure, particularly relevant in the context of global pandemics.

**Keywords:** *Staphylococcus epidermidis*; Human nasal microbiome; Glyceraldehyde-3-phosphate dehydrogenase (GAPDH); Innate immune defense

## INTRODUCTION


The host immune system has evolved both to tolerate beneficial microbiome and to fend off pathogens. Thus, understanding multi-faceted modes of interactions between microbes, either preexisting or invading, and the host is critical to develop novel strategies for managing infections (1-3).

Ho-Keun Kwon 

<https://orcid.org/0000-0003-3175-0376>

Hyun Jik Kim 

<https://orcid.org/0000-0001-8631-928X>

Sang Sun Yoon 

<https://orcid.org/0000-0003-2979-365X>

### Conflict of Interest

The authors declare no potential conflicts of interest.

### Abbreviations

BALF, bronchoalveolar lavage fluid; BCG, Bacillus Calmette-Guerin; CFU, colony-forming units; GF, germ-free; IAV, influenza A virus; MDCK, Madin-Darby canine kidney; MSA, mannitol salt agar; NALF, nasal lavage fluid; PSM, phenol-soluble modulins; rGAPDH, recombinant GAPDH; SPF, specific pathogen-free; TSA, tryptic soy agar; TSB, tryptic soy broth.

### Author Contributions

Conceptualization: Yoon SS, Kim G; Data curation: Yoon SS, Kim G; Formal analysis: Kim G; Funding acquisition: Yoon SS; Investigation: Yoon SS, Kim G; Methodology: Kim G, Lee Y, You JS, Hwang W, Hwang J, Kim HY, Kim J, Jo A, Park IH, Ali M; Resources: Yoon SS, Kim J, Shin JS, Kwon HK, Kim HJ; Supervision: Yoon SS, Kwon HK, Kim HJ; Validation: Yoon SS, Kim G; Visualization: Kim G; Writing - original draft: Yoon SS, Kim G; Writing - review & editing: Yoon SS, Kwon HK, Kim HJ.

The microbiomes that colonize human epithelial surfaces, including those of the intestines, skin, and respiratory tract, are regulated by mucosal immune defense mechanisms. Recent studies have revealed that human microbiome are not just passive bystanders, but actively impact multiple host functions, particularly in immune systems (2). For instance, some members of the gut microbiome actively enhance host resistance to infectious disease within the intestine (4-8). A variety of mechanisms has been described for how the gut microbiome or its derived factors inhibit colonization by enteric pathogens and fortify immune defenses against pathogenic invaders (9,10). In skin, there are some successful therapeutic outcomes using commensal bacteria to inhibit pathogenic (11) or antibiotic-resistant *Staphylococcus aureus* colonization (12). However, in comparison to gut and skin microbiome studies, the mechanistic basis for how the airway microbiome protects a host against respiratory infections is poorly defined.

Inhaled pathogens including bacteria and respiratory viruses first encounter the host immune system through the nasal passage (13-15), and the microbial characteristics of the airway mucus directly impact initiation of the innate immune response (16). Therefore, understanding the human airway mucus microbiome can offer crucial insights into the defense mechanisms against respiratory infections. Additionally, exploring microbiome-related immune factors can lead to the discovery of new concepts for controlling respiratory infections. Previous studies identified *Staphylococcus epidermidis* as the most abundant constituent of nasal mucus in healthy individuals (17,18) and showed that *S. epidermidis* induced a potent antiviral defense mechanism in the nasal epithelium via interferon-related immune responses (17). Despite the reported beneficial effects of *S. epidermidis* in protecting against infection (17,19), the specific biological functions and molecular mechanisms of its complex interkingdom interactions in host-microbiome-pathogen relationships remain largely unknown.

Increasing evidence highlights that microbiome-derived proteins mediate the host-microbiome relationship. For example, *Staphylococcus* species as the common colonizer in the human nasal cavity confer host protection against airway pathogens by producing a serine protease (19) or phenol-soluble modulins (PSMs) (20) that can selectively kill bacterial pathogens, and a specific strain of *S. lugdunensis* produces a thiazolidine-containing cyclic peptide that can inhibit nasal colonization by *S. aureus in vivo* (21). In addition, host immune responses triggered by other intra- or extra-cellular proteins secreted from commensal bacteria have been studied (19,22), and moonlighting proteins (23), exhibiting two or more unrelated functions, might contribute to host protection against several pathogens (24-26). Despite those promising results, the specific mechanisms through which bacterial proteins influence host immune functions need to be further investigated.

In this study, we identified a unique strain that we named AIT01 (Airway Immune Trainer) among 49 isolates of *S. epidermidis* recovered from the human nasal cavity. The strain was distinct in that it activates host infection resistance against pathogenic bacterial or viral infections. Such an immune-enhancing effect was due to a protein secreted into the extracellular milieu in AIT01 but not in other *S. epidermidis* isolates. Together, our results reveal a novel mode of interaction between a host airway and a nasal symbiotic microbe to impact host infection resistance.

## MATERIALS AND METHODS

### *S. epidermidis* screening

We isolated 49 isolates of *S. epidermidis* from the human nasal cavities of healthy individuals or patients suffering from chronic allergy responses (**Supplementary Table 1**). All isolates were categorized based on their capabilities to produce mucinase and/or protease. Each organism was screened for production of extracellular protease and mucinase by inoculation onto tryptic soy agar (TSA, BD Biosciences, Franklin Lakes, NJ, USA) with 1% skim milk powder (27) and 7.5% agar medium (27) with 1% mucin from porcine stomach (Sigma-Aldrich, St. Louis, MO, USA) as a substrate at 37°C for 24 h. Colonies forming clear halos because of partial hydrolysis of milk casein or mucin were recorded as protease or mucinase producing organisms. The isolates that exhibited the highest (AIT01) or lowest (SE28) protease and mucinase activity were selected for further studies.

### Animal experiments

BLAB/c, wild type specific pathogen-free (SPF) and germ-free (GF) mice, all at age 7–10 wk, were used in this study. SPF mice were obtained from Orient Bio (Seongnam, Korea), and GF mice were generated by the Yonsei University College of Medicine GF mouse facility. All mouse experiments were conducted according to the guidelines provided by the Department of Animal Resources of Yonsei Biomedical Research Institute. The Committee on the Ethics of Animal Experiments at Yonsei University College of Medicine approved this study (Permit number, 2017-0210 and 2018-0246). For the influenza A virus (IAV) infection model, female C57BL/6J (B6) mice aged 7 wk were used, and all experiments were approved by the Institutional Review Board of the Seoul National University College of Medicine (IACUC number 2016-0093). For intranasal delivery, mice were anesthetized intraperitoneally with ketamine-xylzine cocktail and treated with  $10^7$  colony-forming units (CFU) of *S. epidermidis* in 20  $\mu$ l of PBS. *S. epidermidis* culture supernatants, and recombinant GAPDH (rGAPDH) protein were administered in a similar manner. The amount/concentration and treatment duration are stated in each figure legend. To quantify bacterial loads in the upper airway (nasal lavage fluid, NALF) and lower airway (bronchoalveolar lavage fluid, BALF), mice were humanely killed, and the trachea was exposed, cannulated, and lavaged with 800  $\mu$ l of PBS for each airway route. Lavage fluid was plated on TSA to quantify total bacteria and on mannitol salt agar (MSA) (27) to quantify AIT01 or SE28 bacteria. *S. epidermidis* showed no color changes in the medium. This means that mannitol had not been fermented and acid end products had not been produced, contrary to *S. aureus* (28). CFU counts were performed after storing overnight at 37°C in aerobic conditions.

### Airway infection model of *P. aeruginosa* PAO1 and other pathogens

For acute airway infection, mice were anesthetized and intranasally inoculated with approximately  $1$  or  $3 \times 10^7$  CFU of *P. aeruginosa* PAO1 in 40  $\mu$ l of PBS. The survival curves were closely monitored every 2 h. To determine PAO1 bacterial load in the lung, mice were humanely killed, and lungs were removed. Lungs were homogenized in PBS, and serial dilutions were plated on Pseudomonas Isolation Agar (Sigma-Aldrich) to selectively determine the PAO1 cells. Detailed information of the other bacterial pathogens is listed in **Supplementary Table 2**.

### In vitro co-culture

*P. aeruginosa* PAO1 ( $10^5$  CFU/ml) was co-cultured in tryptic soy broth (TSB) with each *S. epidermidis* strain ( $10^5$  CFU/ml) for 4, 8, 16, 24, and 36 h. Each strain was enumerated at

each time point by plating serial dilutions of the culture in PBS. *P. aeruginosa* PAO1 was subsequently inoculated ( $10^5$  CFU/ml) into *S. epidermidis* culture supernatants and cultured for 4, 8, 16, 24, and 36 h. *P. aeruginosa* PAO1 CFU was quantified at each time point.

### Bacterial supernatant filtrate preparation

For *in vitro* supernatant culture experiments, *S. epidermidis* strains were cultured aerobically in TSB for 24 h. The bacterial cells in the culture were removed by centrifugation at  $8,000 \times g$  for 10 min at  $4^\circ\text{C}$  and subsequent filtration ( $0.22 \mu\text{m}$ ; Merck Millipore, Seoul, Korea).

### 2-D electrophoresis analysis and identification of the proteins

To further separate the proteins of interest in the *S. epidermidis* culture supernatant, the derived filtrates were precipitated using ice-cold 100% trichloroacetic acid (Sigma-Aldrich). Proteins were quantified by the Bradford assay. Finally, the precipitated proteins, approximately 1 mg, were submitted to Yonsei Proteome Research Center for 2-D electrophoresis analysis.

### Recombinant GAPDH overexpression and purification

The full-length *gapdh* gene from AIT01 was amplified by PCR with primers shown in **Supplementary Table 3**. Detailed information of restriction enzyme is also described in **Supplementary Table 3**. *E. coli* DH5a (Invitrogen, Waltham, MA, USA) was used as the host for plasmid cloning. The *E. coli* BL21(DE3) strain (Novagen) and the pET21a plasmid (Novagen) were used for production of the rGAPDH protein with an N-terminal His6 tag. The rGAPDH proteins were successfully expressed with isopropyl- $\beta$ -thiogalactoside (1 mM) induction in LB medium for 4 h at  $37^\circ\text{C}$ . After harvesting, the cells were disrupted by sonication, and the proteins were purified by Ni-NTA affinity chromatography by the manufacturer's protocol (Qiagen). Purified proteins were further subjected to high-capacity endotoxin removal resin (Bioneer, Daejeon, Korea). Final elutes were examined for purity on a 12% SDS-PAGE and were confirmed by western blotting. The SDS-PAGE gel fractions were submitted to the Yonsei Proteome Research Center for protein identification.

### Cytokine production measurement in the BALF

ELISA kits for IL-1 $\beta$  and IL-6 (R&D Systems, Minneapolis, MN, USA) were used according to the manufacturer's instructions.

### Mouse lung immune cell isolation and flow cytometry

After the mice were killed, the lungs were perfused with 10 ml of PBS through the left ventricle, removed from the trachea, and cut into small pieces with scissors in a 5 ml E-tube. Lung tissue was transferred into a 5 ml reaction tube containing digestion solution (0.05 mg/mL DNase I (Roche, Basel, Switzerland), 3 mg/mL Collagenase type II (Gibco, Life technologies, Carlsbad, CA, USA), 10% FBS) in RPMI-1640 Medium (Gibco), which was held for 30 min at  $37^\circ\text{C}$  with shaking at 850 rpm. The reaction was stopped by addition of 5 ml of MACS buffer (Biochrom, Holliston, MA, USA; Merck Millipore). The remaining red blood cells were lysed using RBC buffer (BD Biosciences). The resulting single-cell suspensions were separated using a  $70 \mu\text{m}$  cell strainer (Greiner Bio-One, Chonburi, Thailand), washed in PBS, and enumerated. For intracellular cytokine staining, cells were stimulated for 4 h at  $37^\circ\text{C}$  with a cell stimulation cocktail (eBioscience, Cat # 00-4970-93). Live/dead staining was performed with an Aqua Live/Dead stain (1:500, Invitrogen, Cat # L34957). Subsequently, the surface was stained with the following monoclonal Abs: CD45 (1:200, BD, clone 30-F11, Cat # 565478), F4/80 (1:200, BioLegend, clone BM8, Cat # 123114), CD11b (1:200, BioLegend,

clone M1/70, Cat # 101206), CD11c (1:200, BioLegend, clone N418, Cat # 117322), Ly6G (1:200, BioLegend, clone RB6-8C5, Cat # 11-5931-82), and TCR $\beta$  (1:200, BioLegend, clone H57-597, Cat # 109251). Cells were fixed and permeabilized with an IC Fixation Buffer (Invitrogen, Cat # 00-8222-49). Intracellular staining was performed with the following monoclonal Abs: TNF $\alpha$  (1:200, BD, clone MP6-XT22, Cat # 554419) and IL-6 (1:200, BD, clone MP6-XT22, Cat # 554419). All samples were studied using a BD LSRII flow cytometer (BD Biosciences) and analyzed with FlowJo v10. (Tree star). The gating strategy is illustrated in **Supplementary Fig. 1**.

### Viruses and reagents

IAV strain A/Wilson-Smith/1933 H1N1 (IAV A/WS/33; ATCC) was used in this study. Viruses were cultured and titrated using Madin-Darby canine kidney (MDCK) cells according to standard procedures (17).

### Virus inoculation

For infections, IAV (213 pfu in 30  $\mu$ l PBS) was inoculated into WT mice by intranasal delivery. After euthanizing the mice, BALF fluid was obtained from the lungs with 1,000  $\mu$ l 0.5 mM EDTA in PBS after cannulation of the trachea. The BAL fluid was used for measuring secreted protein levels, and a plaque assay was used to determine the viral titer. Mouse lung tissue was also harvested for immunohistochemistry analyses.

### Plaque assay

Virus samples were serially diluted with PBS. Confluent monolayers of MDCK cells in six-well plates were washed twice with PBS and then infected in duplicate with 250  $\mu$ l/well of each virus dilution. The plates were incubated at 37°C for 45 min to facilitate virus adsorption. Following adsorption, a 1% agarose overlay in complete MEM supplemented with TPCK trypsin (1  $\mu$ g/ml) and 1% fetal bovine serum was applied. The plates were incubated at 37°C, and cells were fixed with 10% formalin at two-days post infection.

### Immunohistochemistry and histologic analysis

Lung tissue was fixed in 10% (vol/vol) neutral buffered formalin and embedded in paraffin. Paraffin-embedded tissue slices were stained with H&E or periodic acid–Schiff solution (Sigma). Histopathologic analysis of inflammatory cells in H&E-stained lung sections was performed in a blinded fashion using a semi-quantitative scoring system as previously described (29).

### Statistical analysis

For statistical analysis, the GraphPad Prism software v.8.0 (GraphPad Software, Inc., San Diego, CA, USA). Statistical tests were performed using ANOVA tests with Turkey's or Sidak's comparisons with 95% confidence ( $p < 0.05$ ) or multiple  $t$ -tests with different significance levels. Details are shown in figure legends.

## RESULTS

### *S. epidermidis* AIT01 protects mice against *P. aeruginosa* airway infection

We postulated that the microbiome population in a host upper airway can influence the host susceptibility against airway infection. In our preliminary experiment, GF mice were more susceptible to pathogenic *P. aeruginosa* PAO1 than were SPF mice (**Supplementary Fig. 2**). This

finding suggests that airway infection resistance was compromised due to the absence of commensal microbes. We then assessed the effect of intranasal transplantation of commensal *S. epidermidis* on altering host infection resistance because *S. epidermidis* was identified to be the most dominant indigenous microbial species in the human nasal cavity (17,18). We isolated this species from the human nasal cavity of healthy individuals and patients suffering from chronic allergies (Supplementary Table 1). All isolates were categorized by their proteolytic activities, protease and mucinase, based on the idea that active production of such extracellular enzymes can have a positive effect on colonizing human nasal cavities (30). Detailed information of the isolates and proteolytic activities is described in Supplementary Table 1.

We chose AIT01 and SE28 strains for animal experiments, based on their differential production of mucinase and protease. AIT01 is a strong producer of both, while SE28 is a weak producer (Fig. 1A). The experimental scheme shown in Fig. 1B illustrates how mice were treated with *S. epidermidis* transplantation, followed by PAO1 infection. Mice that received transplantation of AIT01 cells developed a significant resistance to PAO1 infection compared to those who underwent transplantation with an equal number of SE28 cells (Fig. 1C). Our findings demonstrate that the transplantation of two distinct human isolates of the same species resulted in markedly disparate conditions within the airway of an exogenous host. Furthermore, AIT01 showed protective effects in GF mice (Fig. 1D), indicating that the transplantation-induced infection resistance is likely associated with the direct effect of AIT01 cells on the host airway, rather than perturbation of the pre-existing

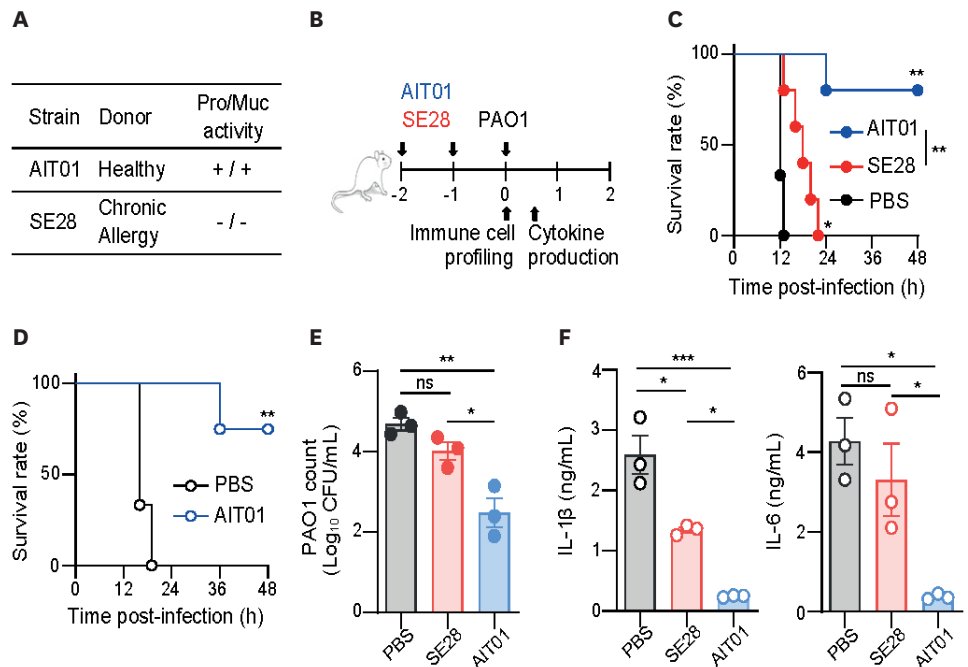


**Figure 1.** AIT01 protects mice against airway *P. aeruginosa* infection. (A) *S. epidermidis* strains used in this study and their proteolytic activities. (B) Experimental scheme. (C) Survival of SPF mice pre-transplanted with  $10^7$  CFU of *S. epidermidis* cells challenged intranasally with  $3 \times 10^7$  CFU of PAO1 ( $n=3-5$  per group). (D) Survival of GF mice pre-transplanted with  $10^7$  CFU of *S. epidermidis* AIT01 challenged intranasally with  $10^7$  CFU of PAO1 ( $n=3$  per group). Mice survival was monitored every 2 h for a total of 2 days and was compared using the log-rank (Mantel-Cox) test. (E) PAO1 burden and (F) cytokine levels (left panel; IL-1 $\beta$ , right panel; IL-6) in BALF at 12 h post-intranasal PAO1 infection. Indicated groups were intranasally administered  $10^7$  CFU of *S. epidermidis* or PBS as a negative control prior to  $10^6$  CFU of PAO1 challenge (mean  $\pm$  SEM,  $n=3$  per group). Pro, protease; Muc, mucinase; +, positive; -, negative; ns, not significant. \* $p < 0.05$ , \*\* $p < 0.01$ , \*\*\* $p < 0.001$ .

airway microbiome. In a separate set of experiments, mice were sacrificed at 12 h post-infection to analyze contents in BALF. The number of PAO1 cells recovered from the AIT01-transplanted group was significantly smaller than that recovered from the SE28-transplanted or control group (Fig. 1E). This finding implies that the transplantation of AIT01 resulted in the inhibition of PAO1 colonization in the mouse airway during the initial infection phase. Consequently, production of inflammatory cytokines IL-1 $\beta$  and IL-6 was markedly suppressed by pretreatment with AIT01 cells (Fig. 1F). In contrast, SE28 cells only mildly suppressed the production of IL-1 $\beta$  and not that of IL-6 (Fig. 1F). Together, our results demonstrate that a lethal infection of PAO1 was almost completely suppressed in a murine host by transplanting a unique strain of *S. epidermidis*.

**Innate immune response to AIT01 transplantation enhances host defense against PAO1 infection**

To further investigate the effects of AIT01 transplantation, we aimed to examine the impact on the immune response in the mouse lung. Given the observed protective effects within 48 h of transplantation, we specifically focused on analyzing the innate immune cell population. Flow cytometry analysis of the lung-infiltrating cells revealed that neutrophils, monocytes (CD11b<sup>low-high</sup>), dendritic cells, and macrophages (Fig. 2A) were remarkably enriched in lung tissues derived from AIT01-transplanted animals. In contrast, such a dramatic increase in neutrophil population was not induced by SE28 transplantation (Fig. 2A). We also found that a larger number of TNF $\alpha$ -producing cells was present in the AIT01-transplanted group,

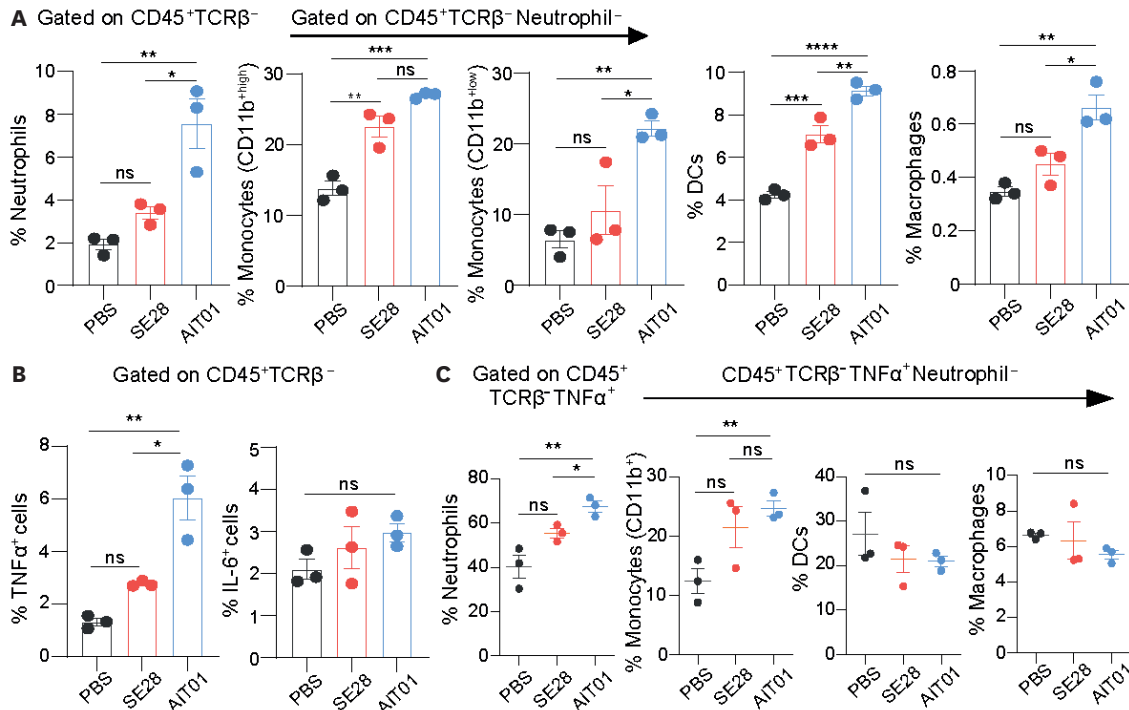


**Figure 2.** AIT01-induced reprogramming of airway immune cells. (A) Flow cytometry of innate immune cells infiltrated in the *S. epidermidis*-administrated mouse lung. (B) Flow cytometry of CD45<sup>+</sup>TCR $\beta$ <sup>-</sup> cells expressing TNF $\alpha$ <sup>+</sup> (left) or IL-6<sup>+</sup> (right) through intracellular staining in mouse lung associated with *S. epidermidis* administration. (C) Flow cytometry of innate immune cells expressing TNF $\alpha$  gated on CD45<sup>+</sup>TCR $\beta$ <sup>-</sup> cells in the mice lung after *S. epidermidis* transplantation. Frequencies of neutrophils (Ly6G<sup>+</sup>CD11b<sup>-</sup>) gated on CD45<sup>+</sup>TCR $\beta$ <sup>-</sup>, and monocytes (CD11b<sup>high</sup> and/or CD11b<sup>low</sup>), dendritic cells (DCs, CD11c<sup>+</sup>F4/80<sup>-</sup>), and macrophages (CD11c<sup>+</sup>F4/80<sup>+</sup>) gated on CD45<sup>+</sup>TCR $\beta$ <sup>-</sup>Neutrophil<sup>-</sup>. Flow cytometry data presented as the mean  $\pm$  SEM (n=3 per group). Statistical differences were assessed by one-way ANOVA with Sidak's test ( $\alpha=0.05$ , n=3). ns, not significant. \*p<0.05, \*\*p<0.01, \*\*\*p<0.001, \*\*\*\*p<0.0001.

while IL-6-producing cells remained largely unchanged (**Fig. 2B**). Cell typing analysis of TNF $\alpha$ -producing cells in the AIT01-transplanted group showed a significant proportion of neutrophils (**Fig. 2C**, far left). Neutrophils accounted for approximately 65% of TNF $\alpha$ -producing cells in the AIT01 group, while the percentages were approximately 40% and 54% in the PBS-treated and SE28-transplanted groups, respectively (**Fig. 2C**, far left). CD11b<sup>+</sup> monocytes were increased in both the SE28 and AIT01-treated animals compared to the PBS-control group (**Fig. 2C**), although there was no significant difference between the two treatment groups. Dendritic cells and macrophages showed similar population levels among TNF $\alpha$ -producing cells in all three groups (**Fig. 2C**). These findings suggest that the elevated presence of innate immune cells, particularly TNF $\alpha$ -producing neutrophils, in the lungs of AIT01-transplanted mice contributes to an enhanced host defense against PAO1 infection.

### AIT01-induced protection is not mediated by antagonistic microbe-microbe interaction

Before we pursued mechanisms of AIT01-induced effects on host resistance against PAO1 infection, we examined whether such protection was ascribed to the superior transplantation capability of AIT01 over SE28. To address this, we counted the number of bacterial cells recovered in NALF samples. At 24 h after transplantation, similar numbers of AIT01 (blue circles) or SE28 (red circles) cells were enumerated on MSA plates in the corresponding transplantation group (**Fig. 3A**). Interestingly, when a different aliquot from the same preparation was inoculated on TSA plates (on which potentially all bacteria cells could grow), comparable numbers of CFU were counted (**Fig. 3A**, black circles). This result indicates that *S. epidermidis* cells in the NALF samples were from the transplanted cells. Consistent with this, colonies of *S. epidermidis* were not detected in the PBS-treated control group (**Fig. 3A**). Mouse body weight did not change for up to 48 h following transplantation (**Fig. 3B**). Importantly, AIT01 or SE28 cells did not induce any increase in production of IL-1 $\beta$  and IL-6 when abundantly present in mouse airway following transplantation (**Fig. 3C**). Delivery of an equal number of PAO1 cells, on the other hand, resulted in robust production of these two cytokines (**Fig. 3C**). These results show that AIT01 and SE28 were equally capable of colonizing the mouse airway, and neither strain showed harmful effects for the host.

Our result shown in **Fig. 1E** indicates that PAO1 cell count was markedly reduced in AIT01-transplanted mice. We therefore asked whether AIT01, but not SE28, would suppress PAO1 growth via direct bacterial competition. When a 1:1 mixture of AIT01 and PAO1 was grown in TSB, PAO1 cells grew normally, while AIT01 cells died (**Fig. 4A**). At 36 h post-inoculation, the CFU of AIT01 cells decreased to  $\sim 10^5$ , the original inoculum size. Likewise, PAO1 grew without interruption in the presence of SE28 cells (**Fig. 4B**). When grown with PAO1, SE28 maintained its viability significantly better than did AIT01. In addition, PAO1 cells grew freely in the culture supernatant of AIT01 or SE28 (**Fig. 4C**), suggesting that PAO1 growth was not affected by secretory molecules of either *S. epidermidis* strain. Together, these results demonstrate that suppression of PAO1 proliferation inside the AIT01-transplanted mouse airway is not a consequence of bacterial rivalry.

### Identification of GAPDH in AIT01 secretory proteome

Next, we investigated mechanisms by which transplanted AIT01 cells rendered the host resistant to PAO1 infection. When pretreated daily with 1  $\mu$ g of AIT01 concentrated culture supernatant (CCS) for 2 days, mice developed robust resistance to the lethal PAO1 infection (**Fig. 5A**, solid blue line). However, such protection was not detected in animals pretreated with 0.1  $\mu$ g of AIT01 CCS (**Fig. 5A**, dotted blue line). Interestingly, CCSs derived from the



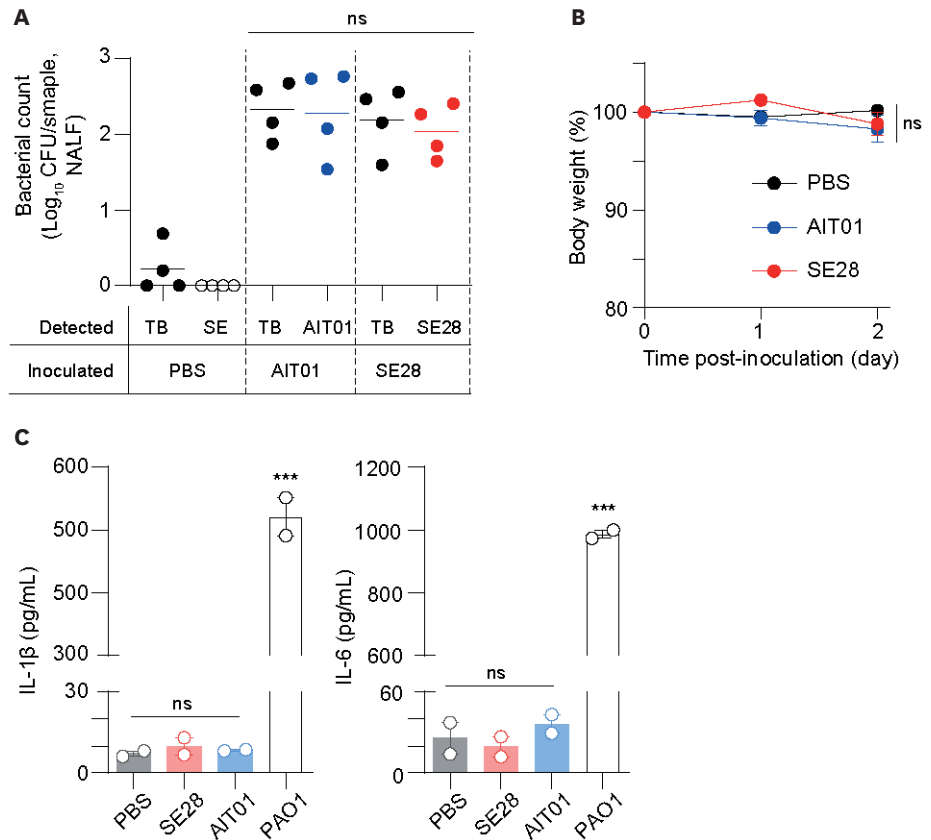


**Figure 3.** Transplantation of *S. epidermidis* cells into mouse airway occurred equally well without any harmful effects. (A) The number of bacterial cells recovered in NALF after 24 h transplantation of *S. epidermidis*. MSA medium was used to selectively cultivate *S. epidermidis* cells with no color change. TB, total bacteria; SE, *S. epidermidis*. (B) Mouse body weight did not change for up to 48 h following transplantation. (C) Cytokine levels in BALF at 12 h post-intranasal inoculation of *S. epidermidis*. Indicated groups were intranasally administered *S. epidermidis* ( $10^6$  CFU) or PBS as a negative control prior to  $10^6$  CFU of PAO1 infection (n=3 per group). ns, not significant. \*\*\*p<0.001.

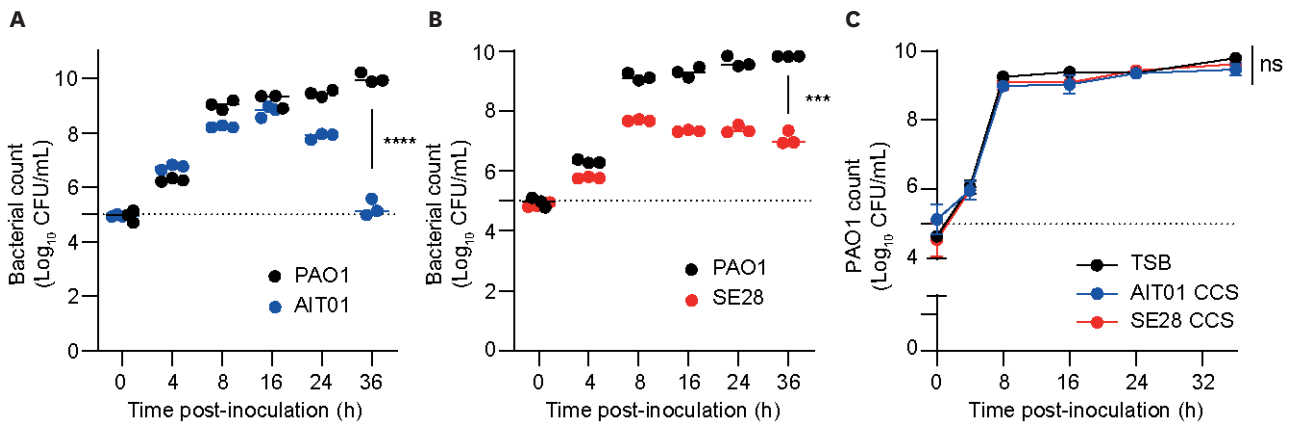


**Figure 4.** PAO1 was not suppressed by co-culturing with *S. epidermidis* cell or its secreted contents. Dual-species growth and bacterial maintenance were determined in a TSB co-culture system. (A) AIT01 (blue circle) and PAO1 (black circle) viable cell counts at 0, 4, 8, 16, 24, and 36 h post-inoculation. (B) SE28 (red circle) and PAO1 (black circle) viable cell counts at 0, 4, 8, 16, 24, and 36 h post-inoculation. Bacterial viability and strain ratios were evaluated at every time point. (C) Growth curve of PAO1 cells in AIT01 or SE28 CCS at 0, 8, 16, 24, and 32 h post-inoculation. ns, not significant. \*\*\*p<0.001, \*\*\*\*p<0.0001.

SE28 cultures failed to protect the host from the same infection (Fig. 5A, red lines). Of note, infection resistance in mice was not fully induced by heat-inactivated AIT01 CCS (Fig. 5B). These results suggest that AIT01 promoted resistance against PAO1 infection in a dose-dependent manner, probably due to heat-labile secretory protein(s).

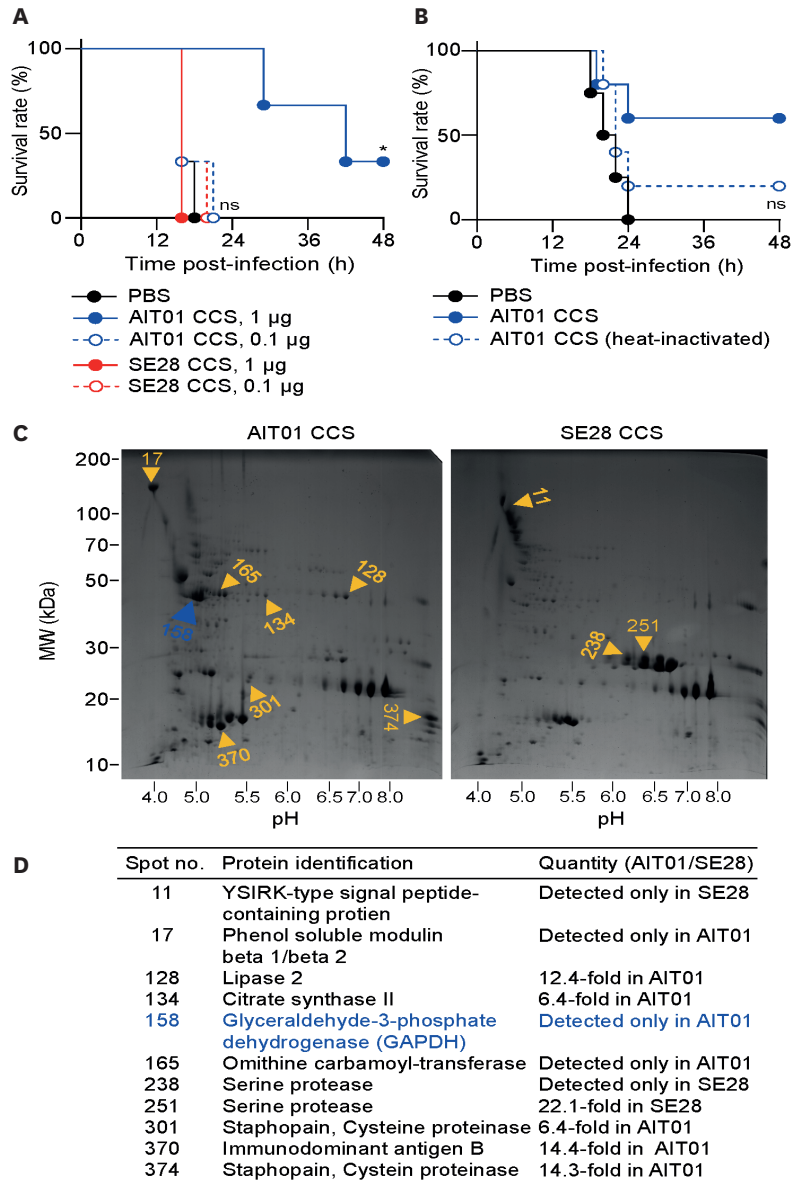


**Figure 5.** Identification of GAPDH in the AIT01 CCS as an immunostimulatory protein. (A) Survival of SPF mice dose-dependently immunized with AIT01 CCS or SE28 CCS after intranasal challenge with PAO1. (B) Survival of SPF mice immunized with AIT01 CCS or heat-inactivated AIT01 CCS after intranasal challenge with PAO1. Mouse survival was monitored every 2 h, and groups were compared using the log-rank (Mantel-Cox) test (n=3-4 mice per group).  $3 \times 10^7$  CFU were used for PAO1 infection. (C) 2-D gel analysis of secreted proteins. Equivalent amounts of secreted protein from AIT01 or SE28 were loaded in a 2-D gel. Protein spots that were differentially synthesized in two strains were identified and labeled with unique numbers. (D) The protein spots marked by arrows in 2-D gel images were identified by mass spectrometry. Quantities of up-regulated proteins (AIT01/SE28) was analyzed by Image Master Platinum 5.0 image analysis program (Amersham Biosciences). ns, not significant. \*p<0.05.

In order to investigate the potential mechanisms behind the observed protective effects of AIT01 transplantation, we conducted a comparison of the secretory proteomes of AIT01 and SE28 using 2-dimensional gel analysis. As shown in **Fig. 5C**, we identified a large spot (spot #158, indicated by blue arrow) that was exclusively present in the AIT01 CCS and not in the SE28 counterpart. Given the size of this spot, we further identified this protein and found it to be GAPDH, a well-known bacterial moonlighting protein with multiple functions (23). We initially found it surprising to observe GAPDH, an intracellular glycolytic enzyme, in such high abundance in the bacterial culture supernatant. Interestingly, we also identified citrate synthase II (spot #134) and ornithine carbamoyl-transferase (spot #165), which are also presumed to be intracellular enzymes, among the AIT01 secreted proteins (**Fig. 3D**). These findings suggest that AIT01 may secrete a range of intracellular proteins into the extracellular environment, potentially contributing to its protective effects against PAO1 infection.

### GAPDH treatment elicited comparable changes in host immune profiles to those induced by AIT01 treatment

We then purified the GAPDH protein (rGAPDH) following overexpression in *E. coli* BL21(DE3) cells (**Fig. 6A**). LPS-removed rGAPDH, when transplanted intranasally, completely protected the host from the PAO1 infection (**Fig. 6B**, solid blue line). None of the mice perished following PAO1 infection, while PBS-controlled mice expired within 18 h post-infection (**Fig. 6B**, black line). Similar to the previous finding (**Fig. 5B**), heat-inactivated rGAPDH failed to provide the same host with infection resistance (**Fig. 6B**, dotted blue line), demonstrating that the protein must be active to exert its protective function inside the host airway. Mouse body weight change was not observed following intranasal delivery of the rGAPDH (**Fig. 6C**), suggesting that the protein was not toxic to the host.

We next explored whether the alterations in immune cell population were induced by purified rGAPDH alone. The TCR $\beta$ <sup>-</sup> cell population significantly increased in rGAPDH-pretreated mice (**Fig. 6D**). Concomitantly, the TCR $\beta$ <sup>+</sup> cell subpopulation decreased in the same group of mice (**Fig. 6D**). These two results suggest that rGAPDH can stimulate the migration of innate immune cells into the host airway. Among TCR $\beta$ <sup>-</sup> cells, Ly6G<sup>+</sup>CD11b<sup>+</sup> neutrophil population was considerably upregulated (**Fig. 6E**). On the other hand, CD11b<sup>+</sup> monocytes, dendritic cells, and macrophages populations were not increased by the same treatment (**Supplementary Fig. 3A**). Importantly, TNF $\alpha$ -producing neutrophils among CD45<sup>+</sup>TCR $\beta$ <sup>-</sup> TNF $\alpha$ <sup>+</sup> cells were elevated in response to treatment with rGAPDH (**Fig. 6F**), but not in the other innate immune cells (**Supplementary Fig. 3B**).

### AIT01 rGAPDH protects the host against infections by Gram-negative pathogens and influenza virus

Although PAO1 has been used as a model infectious agent in experiments to date, our findings suggest that rGAPDH-induced activation of airway immunity may also confer protection against other pathogens. To address this, we additionally tested the 4 bacterial pathogens; *Streptococcus pneumoniae*, *S. aureus*, *Klebsiella pneumoniae*, and *Acinetobacter baumannii*. In each set, bacterial suspensions of 10<sup>6</sup> CFU cells were used for infection. Prior to infection, mice were treated with 2  $\mu$ g of rGAPDH or PBS twice at 24 h intervals. At 24 h post-infection, CFU of *S. pneumoniae* were slightly higher in rGAPDH-treated vs. PBS-control group (**Fig. 7A**). Of note, significantly increased bacterial CFU were observed in both groups, demonstrating that *S. pneumoniae* proliferated well inside the mouse airway. As shown in **Fig. 7B**, two animal groups eradicated *S. aureus* infections in similar ways. While similar numbers of *S. aureus* cells were recovered at 24 h after infection, the bacterial CFU were substantially smaller

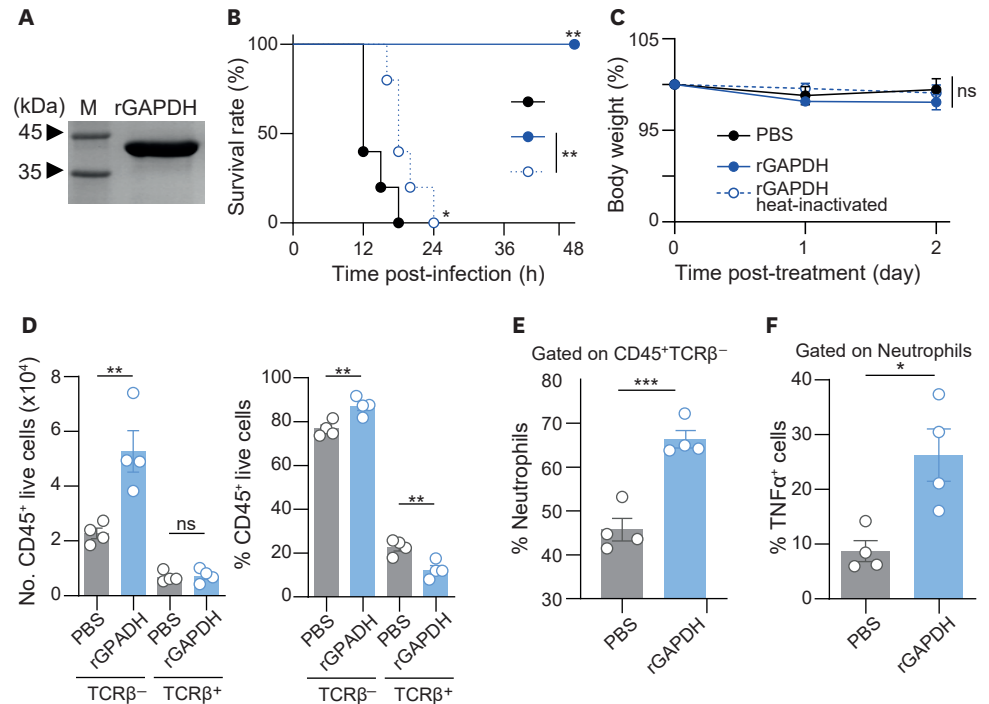


**Figure 6.** AIT01 rGAPDH fortifies host airway innate immunity. (A) Coomassie blue staining of 12% SDS-PAGE gel showing the purified AIT01 rGAPDH. M; protein marker. (B) Survival of SPF mice pre-treated with 2 μg of rGAPDH challenged intranasally with  $3 \times 10^7$  CFU of PAO1 (n=5 per group). Mouse survival was monitored every 2 h for a total of 2 days and was compared using the log-rank (Mantel-Cox) test. (C) Mouse body weight was recorded daily prior to PAO1 infection (n=5 per group). (D) Flow cytometric analysis of TCRβ<sup>-</sup> or TCRβ<sup>+</sup> cells infiltrated into the rGAPDH-treated mice lung. Absolute number of cells (middle panel) and frequencies (right panel) of TCRβ<sup>-</sup> or TCRβ<sup>+</sup> cells are gated on CD45<sup>+</sup> live cells. (E) Flow cytometry analysis of neutrophils (Ly6G<sup>+</sup>CD11b<sup>+</sup>) infiltrated into the rGAPDH-treated mouse lungs; frequencies of neutrophils (Ly6G<sup>+</sup>CD11b<sup>+</sup>) gated on CD45<sup>+</sup>TCRβ<sup>-</sup> cells. (F) Flow cytometry of neutrophils expressing TNFα<sup>+</sup> gated on CD45<sup>+</sup>TCRβ<sup>-</sup> cells; frequencies of neutrophils (Ly6G<sup>+</sup>CD11b<sup>+</sup>) gated on CD45<sup>+</sup>TCRβ<sup>-</sup> cells. Flow cytometry data presented as the mean ± SEM (n=4 per group). Statistical differences were assessed by unpaired t-test.

ns, not significant.  
\*p<0.05, \*\*p<0.01, \*\*\*p<0.001.

than those of *S. pneumoniae*. Taken together, these results suggest that rGAPDH treatment did not have a beneficial protective effect against infections by the two Gram-positive pathogens.

On the other hand, rGAPDH treatment was effective against infections by Gram-negative pathogens. At 16 h post-infection, viable cell numbers of *K. pneumoniae* were ~10-fold smaller in mice pretreated with rGAPDH than in the control group (Fig. 7C). Likewise, *A. baumannii* CFU were reduced more than 10-fold in lungs of rGAPDH-pretreated vs. PBS-control mice (Fig. 7D). Compared with *K. pneumoniae* and *A. baumannii*, PAO1 multiplied robustly inside the mouse airway (Fig. 7E). In the PBS-control group, PAO1 CFU increased to ~10<sup>8</sup> cells during the 12 h infection period, whereas *K. pneumoniae* and *A. baumannii* CFU were ~10<sup>4</sup> to ~10<sup>5</sup> cells. Even in this case, fewer PAO1 cells were recovered in the rGAPDH-treated group (Fig. 7E).

It has been suggested that neutrophils also participate in anti-viral responses (31). Furthermore, TNFα was reported as a key player in anti-influenza response (32). Because TNFα-producing neutrophils were remarkably enriched by AIT01 cell transplantation or by rGAPDH treatment, we hypothesized that rGAPDH treatment would promote an anti-viral response. To address this, mice were infected with IAV following rGAPDH or control treatment. When control mice were infected, body weight gradually decreased, a clear manifestation of IAV-induced

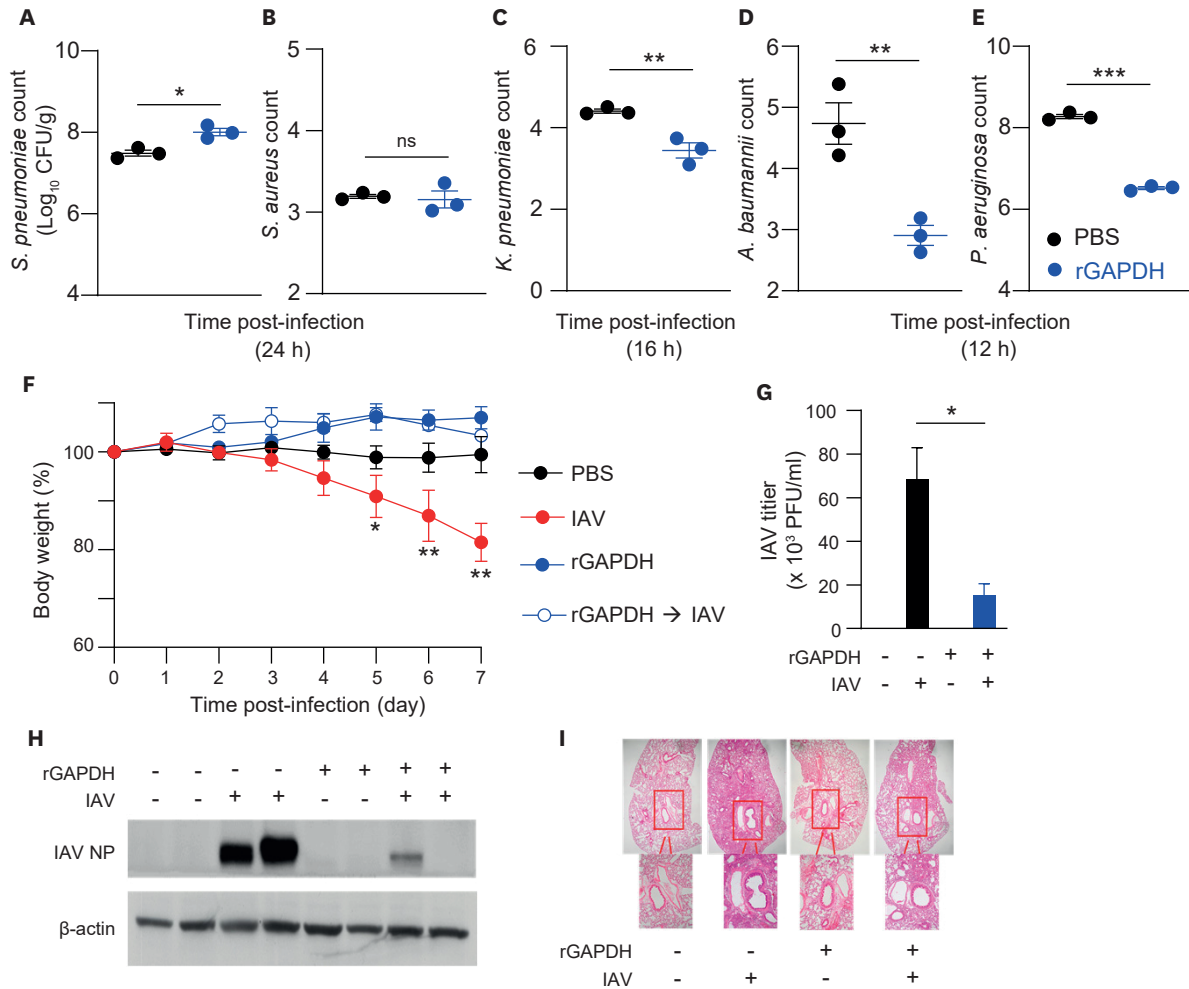


**Figure 7.** AIT01 rGAPDH protects the host against bacterial and viral infection. Burden of Gram-positive (A, B) and Gram-negative bacteria (C, D, E) in mouse lung up to 24 h post-intranasal infection. Indicated groups were intranasally pre-treated with rGAPDH or PBS as a negative control prior to infection of 10<sup>6</sup> CFU of each pathogen (n=3 per group). Data are mean ± SEM. (F) Mean body weight of rGAPDH-treated mice with or without IAV was measured (n=2–4 per group). (G) Viral titer of the infected lung was monitored using plaque assays. (H) Level of IAV nucleoprotein was monitored in the infected lung following IAV infection using western blot analysis. Representative results from two mice in each treatment group are shown. (I) H&E-stained micrographs were generated from lung sections obtained at 7 dpi. ns, not significant. \*p<0.05, \*\*p<0.01, \*\*\*p<0.001.

disease phenotype (**Fig. 7F**, red circle). Such change, however, were not observed in rGAPDH-pretreated mice (**Fig. 7F**, empty blue circle). Treatment with rGAPDH alone did not cause any noticeable changes in mouse body weight, suggesting again that the protein itself had no harmful effect on the host (**Fig. 7F**, blue circle). Moreover, the viral burden was markedly decreased in mice treated with rGAPDH-treated vs. PBS-treated animals (**Fig. 7G**). Detection of the viral nucleoprotein also consistently decreased for the same treatment group (**Fig. 7H**). Most importantly, histopathologic status of the IAV-infected lung was significantly improved in rGAPDH-pretreated mice (**Fig. 7I**). Together, these results demonstrate that rGAPDH, a bacterial moonlighting protein of a symbiont origin, can also protect the host from a deadly viral infection via mechanisms that enhance respiratory immunity.

## DISCUSSION

Recent evidence suggests that *S. epidermidis* colonization plays a crucial role in maintaining tissue homeostasis by modulating the host immune response and preventing colonization by other pathogens (22). However, there are conflicting results, which may be due to the significant strain-level diversity of this species in terms of host immune-modulatory factors. Our study also reveals that two distinct *S. epidermidis* isolates exhibit significantly different host resistance against *P. aeruginosa* infection. Therefore, to utilize *S. epidermidis* as a non-antibiotic treatment or therapeutic agent for pathogenic infections, the strain-level diversity of *S. epidermidis* should be thoroughly understood.

During the *S. epidermidis* screening step, we hypothesized that the proteolytic activities of *S. epidermidis* facilitate successful colonization of the host nasal cavity (30). Using an airway colonization model (17) without antibiotic pre-treatment, we compared the ability of AIT01 and SE28 to colonize the mouse upper respiratory tract. After inoculation of each strain, no differences were found between the two groups (Fig. 3A). Interestingly, however, AIT01 remained well-colonized in the mouse nasal cavity after PAO1 infection, to a greater extent than did SE28 (data not shown), indicating that AIT01 possesses distinct mechanisms for persistent survival in the presence of a pathogenic infection. Pre-existing *S. epidermidis* AIT01, but not SE28, can efficiently secrete GAPDH to recruit activated neutrophils in the mouse lungs, conferring host resistance against invading pathogens. Thus, the ability to rapidly produce and secrete a large amount of GAPDH plays a critical role in maintaining the airway mucosal immunity.

A possible mechanism to explain the significance of *S. epidermidis* strain-level diversity for secreting intracellular proteins is the accessory gene regulator (*agr*) quorum sensing system. The *S. epidermidis agr* regulon controls the production of a small set of potential virulence factors like proteases, lipases, and antimicrobial peptides, and the *agr* system is necessary for adapting quickly to environmental conditions such as in colonizing the skin (33). It will be necessary to ask whether the PSM, a family of amphipathic,  $\alpha$ -helical peptide that was also robustly upregulated in AIT01 supernatant (Fig. 5C and D), is involved in the secretion of GAPDH. It was reported that *agr*-upregulated PSM peptides compromise the membrane integrity of *S. epidermidis* cells, leading to the secretion of intracellular proteins (30,34). This suggests that secretion of AIT01 GAPDH is likely associated with concomitant PSM secretion. Of note, GAPDH associated on the cell surface of *S. epidermidis* has been reported to capture plasminogen, imparting proteolytic activity to the protein and degrading the extracellular matrix, resulting in invasive colonization of host tissue (23,35). In light of our results and these previous findings, GAPDH, as a moonlighting protein, may perform variable functions, depending on whether it is fully secreted from or associated with its host cell.

Our study fits within an emerging field of immunology, termed “trained immunity,” wherein the commensal microbes train host innate immunity and enables a more efficient defense. The concept of trained immunity is based on the observation that certain infections or vaccinations can lead to increased innate immune responses, leading to a more robust response upon subsequent challenges (36). In this study, we propose that pre-exposure to AIT01 or its secreted protein, GAPDH, can prime neutrophils and monocytes to mount more robust responses to subsequent infections. We hypothesize that a particular *S. epidermidis* strain can colonize and train innate immune cells at nasal mucosal barriers, thereby strengthening the first line of defense.

Zymosan, an insoluble  $\beta$ -1,3-glucan extracted from yeast cell wall, efficiently protected host against bacterial infections, including pathogenic *E. coli*, *S. aureus*, *Citrobacter rodentium*, and *P. aeruginosa* PAO1 by increasing Ly6C<sup>high</sup> inflammatory monocytes and granulocytes for up to 5 wk (37). In line with this finding, AIT01 GAPDH also greatly increased pro-inflammatory activity of neutrophils and monocytes that control infections by Influenza virus and Gram-negative pathogens (31). For unclear reasons, however, GAPDH-induced immune activation failed to manage infections by gram-positive bacteria (Fig. 7A and B). In agreement with these results, Ly6G<sup>+</sup> neutrophils were not effective in controlling *Listeria monocytogenes*, a gram-positive intracellular bacterium (37,38). These results strongly suggest that different neutrophil cell types make distinct contributions to immune responses against either Gram-negatives or Gram-positives.

Bacillus Calmette-Guerin (BCG), a tuberculosis vaccine, is another example of a bacterial agent that induces trained immunity. Remarkably, it provides non-targeted protective effects against viral and bacterial infections and exerts anti-tumor effects by enhancing neutrophil activity (39,40). Neutrophils trained by BCG vaccination exhibit (i) enhanced efficacy in killing the fungal pathogen *Candida albicans*, (ii) increased ROS production, and (iii) upregulated expression of degranulation markers (40). Therefore, it will be important to compare the immune-training capability of GAPDH with those of Zymosan and BCG.

In summary, our study has uncovered a novel mechanism through which *S. epidermidis* AIT01 or its GAPDH can modify the host's innate immune response to multiple airway infections, by enhancing neutrophil infiltration and TNF $\alpha$  production. These findings highlight the beneficial effect of pre-existing airway commensal microbiome on promoting host infection resistance. Our data suggest that AIT01 GAPDH could serve as a therapeutic agent for modulating innate defenses in the lung. This approach may offer an alternative to microbiome transplantation for enhancing immune system development and overcoming associated complications.

## ACKNOWLEDGEMENTS

This work was supported by grants from the National Research Foundation of Korea (NRF) grant funded by the Korean Government (2022R1A2C1091845 and 2022M3A9F3017506). This work was supported by the National Research Foundation of Korea (NRF) grant funded by the Korea government (MSIT) (2022R1A2C2011867 and awarded to HJK). This research was also supported by a grant from the Korean Health Technology Research and Development Project through the Korean Health Industry Development Institute, funded by the Ministry of Health and Welfare of the Republic of Korea (HI23C0795 awarded to HJK). This research was supported by the National Research Foundation of Korea (NRF-2022M3A9I2017587).

## SUPPLEMENTARY MATERIALS

### Supplementary Table 1

*Staphylococcus epidermidis* clinical isolates from human nasal cavity and their proteolytic activities, related to Figure 1A

[Click here to view](#)

### Supplementary Table 2

Bacterial strains used in this study

[Click here to view](#)

### Supplementary Table 3

Primers used in this study

[Click here to view](#)

### Supplementary Figure 1

Gating strategy for immune cell analysis in mouse lung. (A) Gating strategy for live CD45<sup>+</sup> cells. (B) Gating strategy for live CD45<sup>+</sup>TCRβ<sup>+</sup> cells. (C) Gating strategy for Neutrophils (CD45<sup>+</sup>TCRβ<sup>+</sup>CD11b<sup>+</sup>Ly6G<sup>+</sup>). Gating for the different innate immune cell subsets pre-gated on live CD45<sup>+</sup>TCRβ<sup>+</sup>Neutrophil<sup>+</sup> cells: Monocytes (D, CD11b<sup>+</sup>); Dendritic cells (E; Q3, CD11c<sup>+</sup>); Macrophages (E; Q2, F4/80<sup>+</sup>).

[Click here to view](#)

### Supplementary Figure 2

GF mice are more sensitive to PAO1 infection than are SPF mice. Survival curve of GF and SPF mice following PAO1 intranasal infection. When administered 10<sup>7</sup> CFU of PAO1, GF mice (n=3) died within 20 h, whereas SPF mice (n=3) survived for 24 h. Log-rank (Mantel-Cox) test.

[Click here to view](#)

### Supplementary Figure 3

Flow cytometry analysis of other innate immune cells, related to **Figure 6E and F**. (A) Flow cytometry analysis of other innate immune cells that are infiltrated in the AIT01 rGPADH-treated mice lung. Frequencies of monocyte (CD11b<sup>+</sup>, left), dendritic cells (CD11c<sup>+</sup>, middle), and macrophages (F4/80<sup>+</sup>, right) within gated on CD45<sup>+</sup>TCRβ<sup>+</sup>Neutrophil<sup>+</sup>. (B) The percentage of the different immune cell subsets producing TNFα gated on CD45<sup>+</sup>TCRβ<sup>+</sup>Neutrophil<sup>+</sup> cells in the mice lung after 24 h of PBS or AIT01 rGAPDH treatment. Statistical differences were assessed by Student's *t*-test. Data are mean ± SEM (n=4 per group).

[Click here to view](#)

## REFERENCES

1. Ruff WE, Greiling TM, Kriegel MA. Host-microbiota interactions in immune-mediated diseases. *Nat Rev Microbiol* 2020;18:521-538.  
[PUBMED](#) | [CROSSREF](#)
2. Zheng D, Liwinski T, Elinav E. Interaction between microbiota and immunity in health and disease. *Cell Res* 2020;30:492-506.  
[PUBMED](#) | [CROSSREF](#)
3. Belkaid Y, Hand TW. Role of the microbiota in immunity and inflammation. *Cell* 2014;157:121-141.  
[PUBMED](#) | [CROSSREF](#)
4. Littman DR, Pamer EG. Role of the commensal microbiota in normal and pathogenic host immune responses. *Cell Host Microbe* 2011;10:311-323.  
[PUBMED](#) | [CROSSREF](#)



5. Hill DA, Artis D. Intestinal bacteria and the regulation of immune cell homeostasis. *Annu Rev Immunol* 2010;28:623-667.  
[PUBMED](#) | [CROSSREF](#)
6. Becattini S, Taur Y, Pamer EG. Antibiotic-induced changes in the intestinal microbiota and disease. *Trends Mol Med* 2016;22:458-478.  
[PUBMED](#) | [CROSSREF](#)
7. Dethlefsen L, Relman DA. Incomplete recovery and individualized responses of the human distal gut microbiota to repeated antibiotic perturbation. *Proc Natl Acad Sci U S A* 2011;108 Suppl 1:4554-4561.  
[PUBMED](#) | [CROSSREF](#)
8. You JS, Yong JH, Kim GH, Moon S, Nam KT, Ryu JH, Yoon MY, Yoon SS. Commensal-derived metabolites govern *Vibrio cholerae* pathogenesis in host intestine. *Microbiome* 2019;7:132.  
[PUBMED](#) | [CROSSREF](#)
9. Khosravi A, Yáñez A, Price JG, Chow A, Merad M, Goodridge HS, Mazmanian SK. Gut microbiota promote hematopoiesis to control bacterial infection. *Cell Host Microbe* 2014;15:374-381.  
[PUBMED](#) | [CROSSREF](#)
10. McKenney PT, Pamer EG. From hype to hope: the gut microbiota in enteric infectious disease. *Cell* 2015;163:1326-1332.  
[PUBMED](#) | [CROSSREF](#)
11. Parlet CP, Brown MM, Horswill AR. Commensal staphylococci influence *Staphylococcus aureus* skin colonization and disease. *Trends Microbiol* 2019;27:497-507.  
[PUBMED](#) | [CROSSREF](#)
12. Nakatsuji T, Chen TH, Narala S, Chun KA, Two AM, Yun T, Shafiq F, Kotol PF, Bouslimani A, Melnik AV, et al. Antimicrobials from human skin commensal bacteria protect against *Staphylococcus aureus* and are deficient in atopic dermatitis. *Sci Transl Med* 2017;9:eaah4680.  
[PUBMED](#) | [CROSSREF](#)
13. Khan R, Petersen FC, Shekhar S. Commensal bacteria: an emerging player in defense against respiratory pathogens. *Front Immunol* 2019;10:1203.  
[PUBMED](#) | [CROSSREF](#)
14. Brown RL, Sequeira RP, Clarke TB. The microbiota protects against respiratory infection via GM-CSF signaling. *Nat Commun* 2017;8:1512.  
[PUBMED](#) | [CROSSREF](#)
15. Ichinohe T, Pang IK, Kumamoto Y, Peaper DR, Ho JH, Murray TS, Iwasaki A. Microbiota regulates immune defense against respiratory tract influenza A virus infection. *Proc Natl Acad Sci U S A* 2011;108:5354-5359.  
[PUBMED](#) | [CROSSREF](#)
16. Zanin M, Baviskar P, Webster R, Webby R. The interaction between respiratory pathogens and mucus. *Cell Host Microbe* 2016;19:159-168.  
[PUBMED](#) | [CROSSREF](#)
17. Kim HJ, Jo A, Jeon YJ, An S, Lee KM, Yoon SS, Choi JY. Nasal commensal *Staphylococcus epidermidis* enhances interferon- $\lambda$ -dependent immunity against influenza virus. *Microbiome* 2019;7:80.  
[PUBMED](#) | [CROSSREF](#)
18. Liu Q, Liu Q, Meng H, Lv H, Liu Y, Liu J, Wang H, He L, Qin J, Wang Y, et al. *Staphylococcus epidermidis* contributes to healthy maturation of the nasal microbiome by stimulating antimicrobial peptide production. *Cell Host Microbe* 2020;27:68-78.e5.  
[PUBMED](#) | [CROSSREF](#)
19. Iwase T, Uehara Y, Shinji H, Tajima A, Seo H, Takada K, Agata T, Mizunoe Y. *Staphylococcus epidermidis* Esp inhibits *Staphylococcus aureus* biofilm formation and nasal colonization. *Nature* 2010;465:346-349.  
[PUBMED](#) | [CROSSREF](#)
20. Cogen AL, Yamasaki K, Sanchez KM, Dorschner RA, Lai Y, MacLeod DT, Torpey JW, Otto M, Nizet V, Kim JE, et al. Selective antimicrobial action is provided by phenol-soluble modulins derived from *Staphylococcus epidermidis*, a normal resident of the skin. *J Invest Dermatol* 2010;130:192-200.  
[PUBMED](#) | [CROSSREF](#)
21. Zipperer A, Konnerth MC, Laux C, Berscheid A, Janek D, Weidenmaier C, Burian M, Schilling NA, Slavetinsky C, Marschal M, et al. Human commensals producing a novel antibiotic impair pathogen colonization. *Nature* 2016;535:511-516.  
[PUBMED](#) | [CROSSREF](#)
22. Laborel-Préneron E, Bianchi P, Boralevi F, Lehours P, Fraysse F, Morice-Picard F, Sugai M, Sato'o Y, Badiou C, Lina G, et al. Effects of the *Staphylococcus aureus* and *Staphylococcus epidermidis* secretomes isolated from the skin microbiota of atopic children on CD4+ T cell activation. *PLoS One* 2015;10:e0141067.  
[PUBMED](#) | [CROSSREF](#)

23. Henderson B, Martin A. Bacterial virulence in the moonlight: multitasking bacterial moonlighting proteins are virulence determinants in infectious disease. *Infect Immun* 2011;79:3476-3491.  
[PUBMED](#) | [CROSSREF](#)
24. Sun X, Wang J, Zhou J, Wang H, Wang X, Wu J, He Y, Yin Y, Zhang X, Xu W. Subcutaneous immunization with *Streptococcus pneumoniae* GAPDH confers effective protection in mice via TLR2 and TLR4. *Mol Immunol* 2017;83:1-12.  
[PUBMED](#) | [CROSSREF](#)
25. Elhaik Goldman S, Dotan S, Talias A, Lilo A, Azriel S, Malka I, Portnoi M, Ohayon A, Kafka D, Ellis R, et al. *Streptococcus pneumoniae* fructose-1,6-bisphosphate aldolase, a protein vaccine candidate, elicits Th1/Th2/Th17-type cytokine responses in mice. *Int J Mol Med* 2016;37:1127-1138.  
[PUBMED](#) | [CROSSREF](#)
26. Feng Y, Pan X, Sun W, Wang C, Zhang H, Li X, Ma Y, Shao Z, Ge J, Zheng F, et al. *Streptococcus suis* enolase functions as a protective antigen displayed on the bacterial cell surface. *J Infect Dis* 2009;200:1583-1592.  
[PUBMED](#) | [CROSSREF](#)
27. Nielsen KL, Olsen MH, Pallejá A, Ebdrup SR, Sørensen N, Lukjancenko O, Marvig RL, Møller K, Frimodt-Møller N, Hertz FB. Microbiome compositions and resistome levels after antibiotic treatment of critically ill patients: an observational cohort study. *Microorganisms* 2021;9:2542.  
[PUBMED](#) | [CROSSREF](#)
28. Ayeni FA, Andersen C, Nørskov-Lauritsen N. Comparison of growth on mannitol salt agar, matrix-assisted laser desorption/ionization time-of-flight mass spectrometry, VITEK® 2 with partial sequencing of 16S rRNA gene for identification of coagulase-negative staphylococci. *Microb Pathog* 2017;105:255-259.  
[PUBMED](#) | [CROSSREF](#)
29. An S, Jeon YJ, Jo A, Lim HJ, Han YE, Cho SW, Kim HY, Kim HJ. Initial influenza virus replication can be limited in allergic asthma through rapid induction of type III interferons in respiratory epithelium. *Front Immunol* 2018;9:986.  
[PUBMED](#) | [CROSSREF](#)
30. Olson ME, Todd DA, Schaeffer CR, Paharik AE, Van Dyke MJ, Büttner H, Dunman PM, Rohde H, Cech NB, Fey PD, et al. *Staphylococcus epidermidis* agr quorum-sensing system: signal identification, cross talk, and importance in colonization. *J Bacteriol* 2014;196:3482-3493.  
[PUBMED](#) | [CROSSREF](#)
31. Camp JV, Jonsson CB. A role for neutrophils in viral respiratory disease. *Front Immunol* 2017;8:550.  
[PUBMED](#) | [CROSSREF](#)
32. Seo SH, Webster RG. Tumor necrosis factor alpha exerts powerful anti-influenza virus effects in lung epithelial cells. *J Virol* 2002;76:1071-1076.  
[PUBMED](#) | [CROSSREF](#)
33. Zhou W, Spoto M, Hardy R, Guan C, Fleming E, Larson PJ, Brown JS, Oh J. Host-specific evolutionary and transmission dynamics shape the functional diversification of *Staphylococcus epidermidis* in human skin. *Cell* 2020;180:454-470.e18.  
[PUBMED](#) | [CROSSREF](#)
34. Tan L, Li SR, Jiang B, Hu XM, Li S. Therapeutic targeting of the *Staphylococcus aureus* accessory gene regulator (agr) system. *Front Microbiol* 2018;9:55.  
[PUBMED](#) | [CROSSREF](#)
35. Henderson B, Martin AC. Protein moonlighting: a new factor in biology and medicine. *Biochem Soc Trans* 2014;42:1671-1678.  
[PUBMED](#) | [CROSSREF](#)
36. Netea M. Trained immunity: a memory for innate host defense. *Eur J Clin Invest* 2019;49:26.
37. Ciarlo E, Heinonen T, Théroude C, Asgari F, Le Roy D, Netea MG, Roger T. Trained immunity confers broad-spectrum protection against bacterial infections. *J Infect Dis* 2020;222:1869-1881.  
[PUBMED](#) | [CROSSREF](#)
38. Shi C, Hohl TM, Leiner I, Equinda MJ, Fan X, Pamer EG. Ly6G+ neutrophils are dispensable for defense against systemic *Listeria monocytogenes* infection. *J Immunol* 2011;187:5293-5298.  
[PUBMED](#) | [CROSSREF](#)
39. Moorlag SJ, Rodriguez-Rosales YA, Gillard J, Fanucchi S, Theunissen K, Novakovic B, de Bont CM, Negishi Y, Fok ET, Kalafati L, et al. BCG vaccination induces long-term functional reprogramming of human neutrophils. *Cell Reports* 2020;33:108387.  
[PUBMED](#) | [CROSSREF](#)
40. Kalafati L, Kourtzelis I, Schulte-Schrepping J, Li X, Hatzioannou A, Grinenko T, Hagag E, Sinha A, Has C, Dietz S, et al. Innate immune training of granulopoiesis promotes anti-tumor activity. *Cell* 2020;183:771-785.e12.  
[PUBMED](#) | [CROSSREF](#)